



Available online at [www.sciencedirect.com](http://www.sciencedirect.com)

**ScienceDirect**

Energy Procedia 91 (2016) 392 – 402

Energy  
**Procedia**

SHC 2015, International Conference on Solar Heating and Cooling for Buildings and Industry

## Novel solar thermal collector systems in polymer design – Part 3: aging behavior of PP absorber materials

Markus Povacz<sup>a</sup>, Gernot M. Wallner<sup>a</sup>, Michael K. Grabmann<sup>a\*</sup>, Susanne Beißmann<sup>b</sup>,  
Klemens Grabmayer<sup>a</sup>, Wolfgang Buchberger<sup>b</sup>, Reinhold W. Lang<sup>a</sup>

<sup>a</sup>University of Linz-Institute of Polymeric Materials and Testing, Altenberger Strasse 69, 4040 Linz, Austria

<sup>b</sup>University of Linz-Institute for Analytical Chemistry, Altenberger Strasse 69, 4040 Linz, Austria

---

### Abstract

A novel, accelerated aging test method was used to characterize the long-term stability of commercial black-pigmented polypropylene (PP) model materials for solar thermal absorbers at elevated temperatures. The PP model materials investigated, PP-B1 and PP-B2, are based on carbon black pigmented PP block copolymer grades. Using an automatized planning technique, sliced 100 µm thick specimens were prepared, aged in hot air and heat carrier fluid (mixture of 60 vol.-% deionized water and 40 vol.-% commercial propylene glycol) at 95°C, 115°C and 135°C for up to 15,000 hours, and characterized in terms of various aging indicators (i.e., remaining primary stabilizer content, oxidation temperature, carbonyl index and ultimate mechanical properties). In general two major trends were discerned. First, the aging processes of the PP compounds depend on the stabilizer system, but even more heavily on the interaction of the stabilizers with the carbon black pigments and the structure and morphology of the polymer. Although the compound PP-B2 exhibited much faster stabilizer loss and an associated drop in oxidation temperature than PP-B1, mechanical investigations proved a better long-term stability for PP-B2. Second, it was shown for the compounds investigated that exposure to hot air causes harsher aging than exposure to hot heat carrier fluid. This is, presumably related to the reduced quantity of dissolved oxygen and triazole-based corrosion inhibitors used in the heat carrier fluid. While PP-B1 is use for absorbers in unglazed collectors and overheating-protected glazed collectors, the investigations clearly revealed that PP-B2 is a promising alternative.

© 2016 The Authors. Published by Elsevier Ltd. This is an open access article under the CC BY-NC-ND license (<http://creativecommons.org/licenses/by-nc-nd/4.0/>).

Peer-review by the scientific conference committee of SHC 2015 under responsibility of PSE AG

**Keywords:** polypropylene; thermal absorbers; aging; long-term stability; flat-plate collector; overheating protection

---

\* Corresponding author. Tel.: +43-732-2468-6620; fax: +43-0732-2468-6613.

E-mail address: [Michael.grabmann@jku.at](mailto:Michael.grabmann@jku.at)

## 1. Introduction

Long-term thermo-oxidative degradation is a major issue for polymers under all environmental conditions [5], especially for those applied in solar thermal applications [15]. Polymers are exposed to elevated temperatures and various surrounding media, such as air and, water or water/glycol mixtures, for long periods of time. In addition, UV-induced photo-oxidation phenomena overlap with thermal aging in terms of temperature effects. Thus, polymers are usually stabilized with antioxidant packages containing processing stabilizers against thermal degradation of the polymer melt during the processing stage and long-term antioxidants and UV stabilizers against degradation in the application stage [7,8]. To assess thermo-oxidative degradation and to predict the lifetime of polymeric materials, various studies have been carried out and methods have been developed [4]. One of the most common approaches to thermal polymer degradation analysis is to correlate degradation chemistry and mechanical properties. Combining high temperatures with an oxygen-rich environment is a convenient means of accelerating the degradation of the polymer. Chemical changes are usually monitored by infrared spectroscopy (e.g. carbonyl index evaluation) [12] and size-exclusion chromatography (e.g. molecular weight analysis) [15] and related to conventional mechanical tests such as tensile or impact tests. Correlations between changing properties determined by, various methods are used for lifetime prediction.

As summarized by Mantell and Davidson [17] in terms of polymeric materials for solar absorber, various aging studies in different media have been performed to investigate polymer durability [9,14,15,18]. Detailed investigations of the aging behavior of unpigmented commodity plastics and various black-pigmented engineering plastics were carried out in hot water and hot air by Kahlen et al. [15]. In this paper we present an alternative approach of thermo-oxidative degradation investigation. We used commercially available carbon black pigmented polypropylene block-copolymer grades as model systems and evaluated their aging behaviors under service conditions relevant to solar thermal applications. The approach is based on micro-sized specimens with enhanced surface-to-volume ratio [19] that results in reduction of diffusion-limited oxidation (DLO) complications [20]. Miniaturization of the specimens made it possible to expose more samples in limited heating oven space. The main goal of our investigations was to obtain an improved understanding of the degradation processes of black-pigmented polypropylene materials for solar absorber applications and to elucidate the effects of different exposure media on the mechanisms of aging.

## 2. Experimental

### 2.1. Materials

The model materials PP-B1 and PP-B2 selected for this work are black-pigmented polypropylene block copolymers. PP-B1 was chosen as a benchmark system because of its wide use in commercially available polymeric solar collectors (e.g. swimming pool absorbers by FAFCO® and by HELIOCOPOL®, and glazed solar absorber Eco-Flare® by Magen Eco-Energy) due to its high heat stability and high extraction stability. Provided by LyondellBasell, Houston, USA it is an extrusion grade with a melt flow rate of 0.3 g/10 min (230°C/2.16 kg). PP-B2, provided by Borealis Polyolefine GmbH, Linz, Austria, is a  $\beta$ -nucleated, heterophasic copolymer grade developed especially for hot-water compression fittings. The carbon black pigmentation offers excellent UV resistance making it a potential candidate for solar thermal absorbers. Samples were prepared by compression moulding of 2 mm thick plates on a mechanical laboratory press. 5A type specimens (ISO 527-2/5A) for tensile testing were machined with a puncher. The micro-sized film-specimens for accelerated aging were automatically processed on a CNC-machine [19]. 100  $\mu\text{m}$  thick film-specimens with a width of 2 mm and a length of 200 mm were sliced from compression-moulded plates.

### 2.2. Basic characterization methods

Various methods were used for basic characterization. Polarizing optical microscopy (POM) in transmitted light mode was employed to determine the spherulitic structure and to assess the dispersion quality of the carbon black

pigmentation in PP-B1 and PP-B2. Microtomed specimens (i.e., slices with 10 µm thickness) were probed using a BX 61 microscope (Olympus Austria GmbH; Vienna, Austria) with 5x and 50x objectives in transmitting mode.

To determine the black pigment contents of the PP grades, thermo-gravimetric analysis (TGA) was performed under inert nitrogen atmosphere using a Perkin Elmer STA 6000 (Perkin Elmer GmbH; Rodgau, Germany). The heating rate was 20 K min<sup>-1</sup>. The residual weight after decomposition of the organic polymer matrix was considered to be carbon black content [6].

Differential Scanning Calorimetry (DSC) was used to characterize the thermal transitions. Samples with a mass of approximately 3 mg were taken from compression-moulded plaques, placed in 30 µl aluminium pans with perforated lids and tested using a Perkin Elmer DSC 4000 (Perkin Elmer GmbH; Rodgau, Germany). Melting point and oxidation temperature were obtained by DSC with heating/cooling rates of 10 K min<sup>-1</sup> under static air purge. The degree of crystallinity of the β-phase of PP-B1 was calculated using an enthalpy of fusion of 100% crystalline α-iPP of 207 J g<sup>-1</sup> [10]. To determine the crystallinity and β-phase content of the β-nucleated PP-B2, also wide-angle X-ray scattering (WAXS) was performed.

The solar-optical properties of 2 mm thick plaques were determined using a Perkin Elmer Lambda 950 spectrophotometer (Perkin Elmer GmbH; Rodgau, Germany) equipped with a Spectralon Ulbricht sphere (diameter of 150 mm). To obtain integral hemispherical absorbance values, normal-hemispherical transmittance and reflectance spectra of the samples were measured, integrated and weighted in steps of 5 nm by the AM 1.5 global solar irradiance source function [3].

The mechanical properties of 5A multi-purpose specimens were investigated by means of dynamic mechanical analysis (DMA) and tensile testing. Information about the temperature dependence of the mechanical properties was gained using a Dynamic Mechanical Analyzer (Type: DMA 8000; Perkin Elmer GmbH; Rodgau, Germany). To determine the storage modulus, E<sub>f</sub>', and the loss factor, tan(δ) in the temperature range from -25°C to 160°C, a single cantilever bending mode was applied with a heating rate of 2°C min<sup>-1</sup>. A screw-driven universal testing machine (Type: Zwick Line Z5.0; Zwick GmbH & Co. KG; Ulm, Germany) with an initial clamping length of 50 mm and a test speed of 50 mm/min was applied to derive stress-strain curves. Ten unaged specimens were tested at ambient temperature to evaluate Young's modulus, E<sub>T</sub>, yield stress, σ<sub>Y</sub>, and strain-at-break, ε<sub>B</sub>. Young's modulus was determined applying a multi-extensometer.

### 2.3. Aging characterization methods

Micro-sized specimens (i.e. slices with 100 µm thickness) were exposed to hot air and heat carrier fluid at temperatures of 95°C, 115°C and 135°C using heating ovens (Type: Binder FED 53; Binder GmbH; Tuttlingen, Germany). To ensure homogeneous aging conditions in air, specimens were fixed to metal grids using sample clips. The heat carrier fluid was a mixture of 40 vol.-% commercially available propylene glycol Tyfocor L and 60 vol.-% deionized water. For exposure to the heat carrier fluid, pressure-resistant stainless steel containers were constructed and manufactured. The heat carrier fluid in the vessels was changed at intervals of about 2,500 h to minimize saturation effects of leached out additives [8,15].

After various stages of aging in hot air and hot heat carrier fluid, the specimens were characterized to obtain information about physical and chemical changes. To examine the stabilizer consumption a validated chromatographic approach was performed, using high-performance liquid chromatography (HPLC) (Type: 1260 Infinity; Agilent Technologies; Santa Clara, USA) equipped with an UV-detection [2]. Differential Scanning Calorimetry (DSC) was applied to evaluate the shift in oxidation temperature. The carbonyl index (C.I.) was determined by FT-IR spectroscopy (Type: Spectrum 100 spectrometer, Perkin Elmer; Rodgau, Germany) in transmittance mode. Normal-normal transmittance spectra were recorded in the wavenumber range from 700 to 4,000 cm<sup>-1</sup> at a resolution of 2 cm<sup>-1</sup> performing an average of 20 scans. The spectra were corrected with regard to variations in sample thickness by normalization with respect to the absorbance peak at 974 cm<sup>-1</sup>. The corresponding CH<sub>3</sub> rocking band remained unchanged during the degradation of the polymer. In contrast, with increasing oxygen uptake the peak relating to carbonyl build-up (C=O stretch band) increased. Subsequently, the C.I. was calculated by the ratio of absorbance peaks at 1,715 cm<sup>-1</sup> (carbonyl-peak) to 974 cm<sup>-1</sup> [12]. By tensile testing (Type: Zwick Line Z2.5; Zwick GmbH & Co. KG; Ulm, Germany) the change in the ultimate mechanical properties such as strain-at-break was evaluated. For each state of aging a minimum of five specimens was tested.

### 3. Results

#### 3.1. Basic characteristics and properties of the PP grades

The microscopic investigations revealed for compound PP-B1 a coarse spherulitic structure with spherulite sizes ranging from 100 to 130  $\mu\text{m}$ , while for the PP-B2 grade no spherulitic structure was detectable by light microscopy. For both grades a well-dispersed carbon black structure with spherical agglomerates with diameters ranging from 0.3 to 0.5  $\mu\text{m}$  was found.

TGA thermograms of PP-B1 and PP-B2 under nitrogen atmosphere exhibited an onset of thermal decomposition at about 455°C for PP-B1 and 440°C for PP-B2. As described by Chrissafis et al. [6], pure polypropylene matrix degrades, while the residual weight (about 2.0 wt.-% for PP-B1 and 0.8 wt.-% for PP-B2) can be related to the amount of carbon black. The content of carbon black in PP-B1 was about two times higher. The DSC thermograms of PP-B1 and PP-B2 are compared in Fig. 1. PP-B1 showed a melting temperature that is characteristic of the  $\alpha$ -phase, with a melting peak at 163°C and a melting enthalpy of 52 J g<sup>-1</sup>, which corresponds to 26% crystallinity. In the oxidation regime, an oxidation temperature of 267°C was determined. For PP-B2, in contrast, two melting peaks were observed, which is characteristic of  $\beta$ -nucleated PP. The first melting peak with a maximum at 148°C is related to the  $\beta$ -phase, while the second peak at 164°C is characteristic of the  $\alpha$ -spherulitic structure. WAXS analysis determined a  $\beta$ -phase content of 91% and an overall degree of crystallinity of 63%. In comparison to PP-B1, the oxidation temperature of PP-B2 shifted towards slightly lower temperatures around 266°C, predominantly resulting from different stabilizer packages.

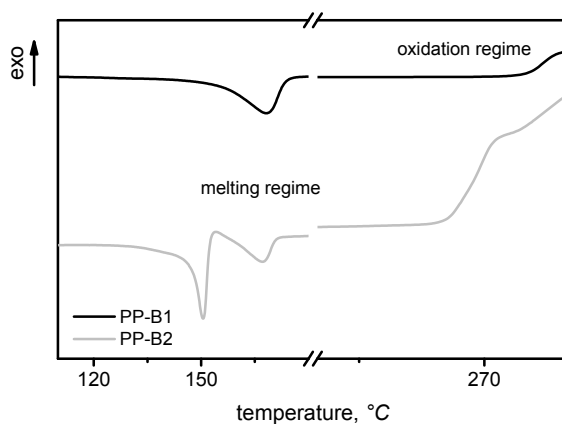


Fig. 1. DSC thermograms of PP-B1 and PP-B2 showing the melting and oxidation regime of the 2nd heating interval.

Fig. 2 illustrates the normal-hemispherical reflectance spectra of the two model materials over the solar wavelength range. In comparison to black-pigmented PP-RCT compounds investigated in previous work [16], PP-B1 and PP-B2 revealed slightly lower solar reflectance of 4.0% and 4.3%, respectively. Since the solar transmittance values of the black plaques were negligible, the solar absorbances of the black-pigmented PP-B1 and PP-B2 plaques were 96.0% and 95.7%.

Fig. 3 plots the DMA thermograms (storage modulus and loss factor). Maxima in the loss factor curves associated with transitions in the storage modulus were observed at 10°C and 30°C for PP-B1 and at 110°C and 90°C for PP-B2. These transitions are attributable to inner material mobility in the amorphous and crystalline phases. The increase in the loss factor and drop in storage modulus at about 160°C is related to melting of the materials. The storage moduli  $E'_t$  of the materials decreased from about 1,500 MPa at ambient temperature to about 250 MPa to 400 MPa at 95°C.

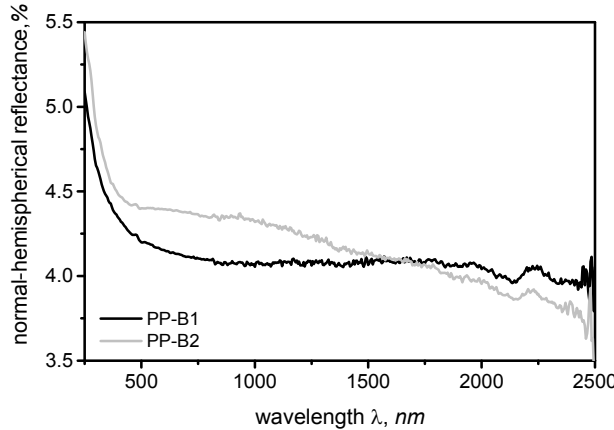


Fig. 2. Normal-hemispherical reflectance spectra for 2 mm thick black pigmented PP-B1 and PP-B2 plaques.

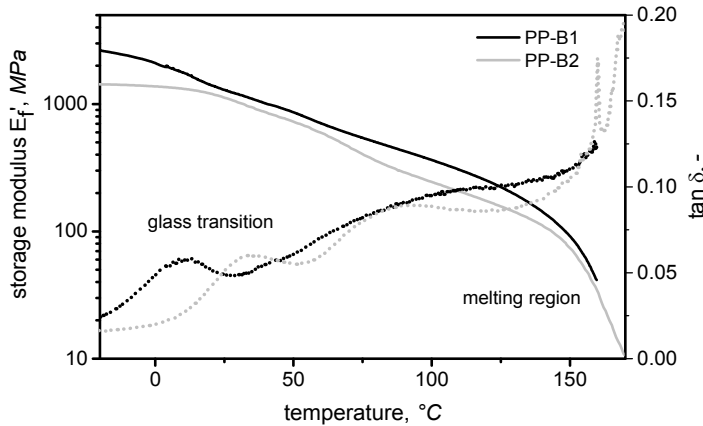


Fig. 3. DMA curves of the investigated polypropylene model materials PP-B1 and PP-B2. The solid curves illustrate the temperature-dependent storage modulus  $E'_f$  and the dotted curves plot the loss factor  $\tan(\delta)$ .

Stress-strain curves from tensile tests illustrate a pronounced necking behavior, starting with a yield point at about 10% strain (Fig. 4). The behavior in the plastic deformation regime was significantly different, with lower strain-at-break values for PP-B1 and pronounced strain hardening for PP-B2 at higher strain values of 300% to 400%. The lower ultimate value and the higher standard deviation of PP-B1 are, presumably, related to the coarse spherulitic structure with a spherulite size equal to the thickness of the specimen. The unaged black-pigmented PP-B1 grade exhibited a slightly lower Young's modulus of 1,370 MPa and a yield stress of 25 MPa. In contrast, the Young's modulus and yield stress values of PP-B2 were 1,510 MPa and 27 MPa, respectively.

### 3.2. Aging behavior

In Figs. 5 to 8 changes in the primary antioxidant content (top layer), the oxidation temperature  $T_{ox}$  (top middle layer), the C.I. (bottom middle layer) and the strain-at-break values (bottom layer) are plotted over the exposure time in hot air (Figs. 5 and 6) and hot heat carrier fluid (Figs. 7 and 8) for PP-B1 and PP-B2. The dotted, dashed and solid curves represent changes in properties observed at 95°C, 115°C, and 135°C.

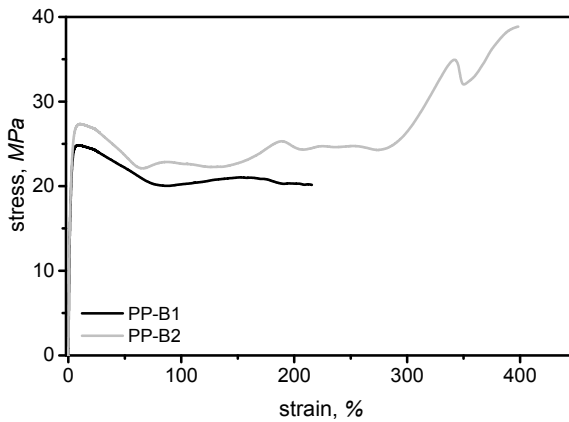


Fig. 4. Stress-strain curves of the investigated 5A specimens of PP-B1 and PP-B2.

#### Aging behavior in hot air

Exposure of PP-B1 and PP-B2 to hot air (Figs. 5 and 6) led at all temperatures to significant consumption of stabilizers, which was described by an exponential function. For PP-B1, the primary antioxidants package reached the lower detection limit of 0.01 wt.-% after 950 hours of exposure to hot air at 135°C, while at 115°C and 95°C this detection limit was reached after approximately 3,200 and 9,000 hours, respectively. Hence, for a temperature difference of 20 K, an acceleration factor for ultimate stabilizer loss of about 3 was obtained. The depicted primary antioxidant values shown include only unconsumed tri- and tetra-functional primary antioxidants. Stabilizer molecules with oxidized functional groups were not considered and evaluated. Nevertheless, the remaining phenolic groups were still active and kept protecting the polymer from thermo-oxidative degradation. Consequently, the effective and true residual primary antioxidant concentration should be higher when accounting for the antioxidant molecules with remaining hindered phenolic groups [8]. In general, the detection limit for PP-B2 was reached by a factor of 2 earlier compared to PP-B1. The significant difference in antioxidant loss is related to the fact, that tri- and tetra-functional phenolic antioxidants were added to PP-B1, while PP-B2 consisted of tetra-functional phenolic antioxidants only.

A significant effect of the exposure temperature on the decrease in oxidation temperatures was observed. The values measured for PP-B1 were fitted to linear functions, which resulted in regression coefficients ( $R^2$ ) of 0.94 to 0.96. For PP-B2 the oxidation temperature levelled off at 220°C. Considering the detection limit values for the primary antioxidants and the changes in oxidation temperature, PP-B1 reaching the antioxidants detection limit agrees with a critical oxidation temperature of 240°C. This same agreement was found for PP-B2 (except at 95°C), but showing a critical oxidation temperature of 220°C.

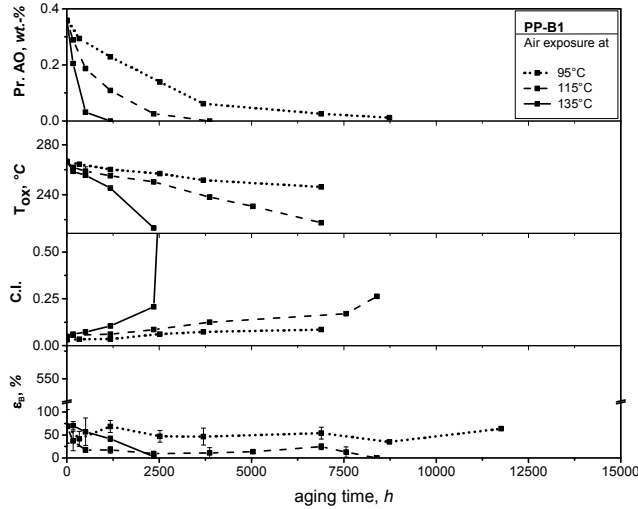


Fig. 5. Primary antioxidant content, oxidation temperature ( $T_{ox}$ ), carbonyl index (C.I.) and strain-at-break ( $\epsilon_B$ ) for black-pigmented PP-B1 micro-sized specimen as functions of aging time in hot air at 95°C, 115°C and 135°C.

In terms of C.I. and strain-at-break as measures of premature failure and embrittlement (s. Figs. 5 and 6), the best behavior was observed for PP-B2 at 95°C hot air exposure. No embrittlement was detected for up to 15,000 hours of exposure. At 115°C and 135°C, the critical strain-at-break values (below yield strain) were reached after 14,000 h and 5,000 h, respectively. The reaching of the critical C.I. and the strain-at-break values does not coincide with the antioxidant detection limit or the time required to reach the critical oxidation temperature of 220°C. Interestingly, PP-B1 exhibited a considerably faster rise in the carbonyl index and significantly lower time-to-embrittlement values. Compared to PP-B2, embrittlement after exposure to 115°C and 135°C was reached in half the time. Hence, it was concluded that the long-term performance is significantly affected also by the morphological structures, including the carbon black content, the crystal form ( $\alpha$  vs.  $\beta$ ) and the crystallinity. Of special relevance are the low carbon black content and the  $\beta$ -phase structure with higher crystallinity values in PP-B2. For the critical carbonyl index and the strain-at-break values an acceleration factor of about 3 was obtained for both grades comparing the data at 115°C and 135°C.

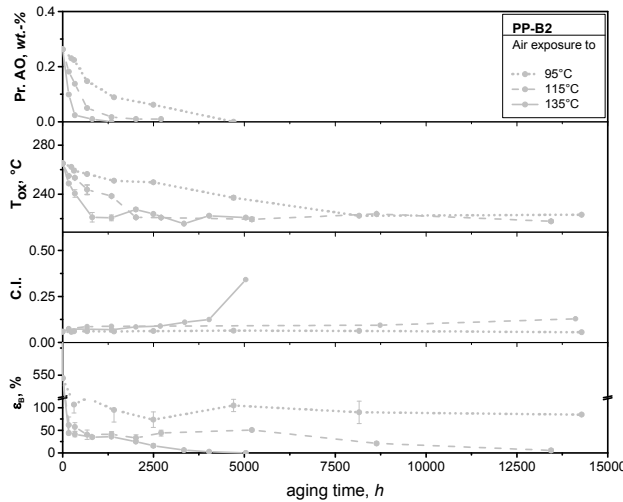


Fig. 6. Primary antioxidant content, oxidation temperature ( $T_{ox}$ ), carbonyl index (C.I.) and strain-at-break ( $\epsilon_B$ ) for black-pigmented PP-B2 micro-sized specimen as functions of aging time in hot air at 95°C, 115°C and 135°C.

### Aging behavior in hot heat carrier fluid

The aging indicators characterized after exposure to hot heat carrier fluid (Fig. 7 for PP-B1 and Fig. 8 for PP-B2) clearly indicate, that the aging conditions in a mixture of 40 vol.-% propylene glycol (Type: Tyfocol L; TYFOROP Chemie GmbH; Hamburg, Germany) and 60 vol.-% deionized water are less aggressive than in hot air for the same temperatures. The influence of the exposure media on the aging behavior of PP-B1 can be seen by comparing Figs. 5 and 7. While the aging behavior in hot air showed a rapid drop in the investigated properties, in hot heat carrier fluid the indicators consumption of primary antioxidants, oxidation temperature and strain-at-break revealed a slower decrease and did not reach critical values. In contrast PP-B2 exhibited small differences. The mechanical long-term behavior of PP-B2 was more constant than for exposure to hot air, although loss of primary antioxidants and decrease in oxidation temperature (both stabilizer-dependent properties) were slightly accelerated.

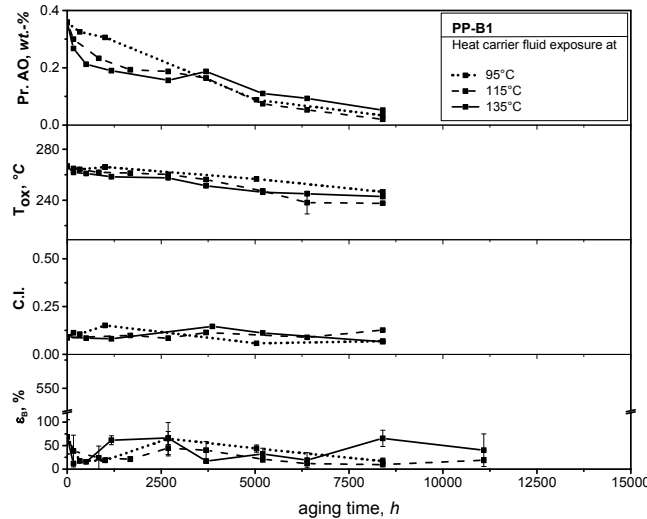


Fig. 7. Primary antioxidant content, oxidation temperature ( $T_{ox}$ ), carbonyl index (C.I.) and strain-at-break ( $\epsilon_B$ ) for black-pigmented PP-B1 micro-sized specimen as functions of aging time in hot heat carrier fluid at 95°C, 115°C and 135°C.

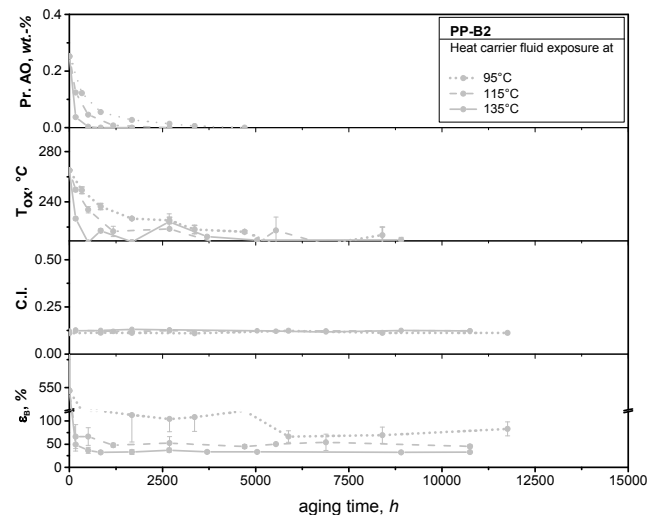


Fig. 8. Primary antioxidant content, oxidation temperature ( $T_{ox}$ ), carbonyl index (C.I.) and strain-at-break ( $\epsilon_B$ ) for black-pigmented PP-B2 micro-sized specimen as functions of aging time in hot heat carrier fluid at 95°C, 115°C and 135°C.

In Fig. 9, the oxidation temperatures are plotted versus the primary antioxidants content. For PP-B1 a linear correlation independent of the medium and the exposure temperature was observed. PP-B2 exhibited also a linear relationship, which was significantly dependent on the medium, but independent on the exposure temperature. The differences are, presumably, related to the formulation of the materials. The tetra-functional long-term antioxidant in PP-B2 is based on ester spacer groups, which are prone to hydrolysis in water/glycol mixtures at elevated temperatures. In contrast, PP-B1 was formulated with more hydrolysis stable primary antioxidants.

The middle top layer of Fig. 7 illustrates that in comparison to high-temperature aging in air (Fig. 5), in the heat carrier medium the decrease in oxidation temperature decelerated at all temperatures. After exposure times of about 8,400 hours to 95°C, 115°C and 135°C the oxidation temperature of the aged films reached about 240°C. Consequently, in the heat carrier fluid the mechanisms for PP-B1 were not affected by temperature variation. For PP-B2, a contrary trend can be observed in Fig. 8, associated with the accelerated stabilizers loss due to leaching and hydrolysis. Here, even a faster decrease in the oxidation temperature was measured, reaching the indicator of 220°C after about 300, 1,000 and 3,000 hours for exposure temperatures of 135°C, 115°C and 95°C.

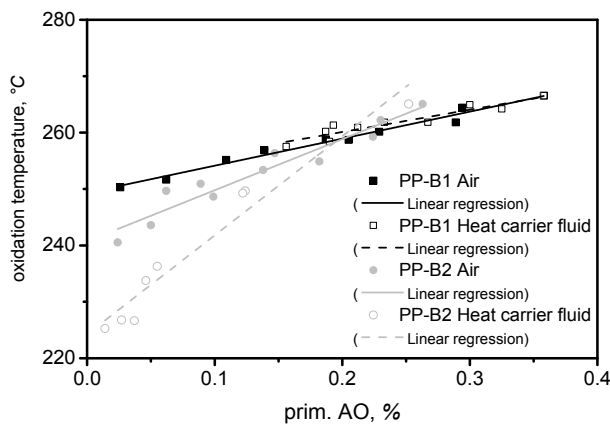


Fig. 9. Linear correlation of primary antioxidant consumption and drop in oxidation temperature ( $T_{ox}$ ) for PP-B1 and PP-B2 after exposure to hot air and hot heat carrier fluid at various temperatures (95°C, 115°C and 135°C).

No significant changes in terms of C.I. and long-term mechanical stability were observed after exposure to hot heat carrier fluid. The pronounced initial drop in the strain-at-break values in the beginning of exposure is related to physical aging. No premature failure occurred in the test period of up to 8,400 hours. The mechanical properties of PP-B1 and PP-B2 were less affected by exposure to hot heat carrier fluid than to hot air. This is in contradiction to findings reported by, for instance, Allen et al. [1] and Dörner and Lang [8]. We presume that the differences are related to the use of triazole-based corrosion inhibitors in the antifreezing and anticorrosion concentrate and the reduced concentration of available oxygen in the pressure vessels. Furthermore, PP-B1 contains stabilizers with greater hydrolytic resistance and low extractability in water. FT-IR spectroscopy measurements revealed a continuous build-up of an additional peak in the region from 1,530 to 1,570 cm<sup>-1</sup> for samples exposed to heat carrier fluid at 135°C (Fig. 10). The peak is attributable to -N-H- bonds and was also detected in the propylene-glycol mixture. Manufacturer's information about the concentrate Tyfocor L attests to the usage of corrosion inhibitors, which are often based on triazole compounds [11]. These chemical compounds are usually added to protect the metal against corrosion. The investigations indicated that triazole based corrosion inhibitors improve the aging performance of the PP-grades.

#### 4. Summary and Conclusions

In this paper two black-pigmented PP grades for solar thermal absorbers were characterized as to their basic properties and the aging behavior under service relevant conditions. PP-B1 exhibited a carbon black content of

about 2 wt.-%, a melting temperature of 163°C and lower ultimate mechanical values attributable to spherulites with diameters of about 100 µm. In comparison, PP-B2 is characterized by a lower carbon black content (0.8 wt.-%) and a lower melting temperature due to its  $\beta$ -crystalline phase structure. For both grades an excellent solar absorbance of 96% was ascertained. Regarding the aging behavior, more pronounced changes were observed after hot air aging. Depending on the stabilizer system used, the detection limits for primary stabilizers were reached after 600 hours and 1,000 hours of hot air exposure at 135°C for PP-B2 and PP-B1. Subsequently, chemical aging phenomena were investigated, manifesting as rapid drop in oxidation temperature and embrittlement of PP-B1 films after 2,350 hours. Although PP-B2 showed a faster decrease in the stabilizer content and oxidation temperature, the long-term mechanical properties were significantly better. This was attributed to lower carbon black content and the  $\beta$ -phase structure of PP-B2. At 115°C, hot air aging decelerated, leading to embrittlement after 8,000 hours and about 13,500 hours for PP-B1 and PP-B2, respectively. In general, all investigated property degradation functions shifted towards flatter decay curves. At 95°C in hot air, no embrittlement was observed for PP-B2 for exposure times of up to 14,000 hours.

When exposed to hot heat carrier fluid, the aging of PP-B1 and PP-B2 is significantly retarded, which was attributable to the uptake of triazole-based corrosion inhibitors, commonly added to solar thermal heat carrier fluids. At all investigated temperatures, no embrittlement of the 100 µm thick films was observed. Compared to hot air aging at 135°C, exposure to heat carrier fluid resulted in a time-to-embrittlement that was by more than a factor 4 longer.

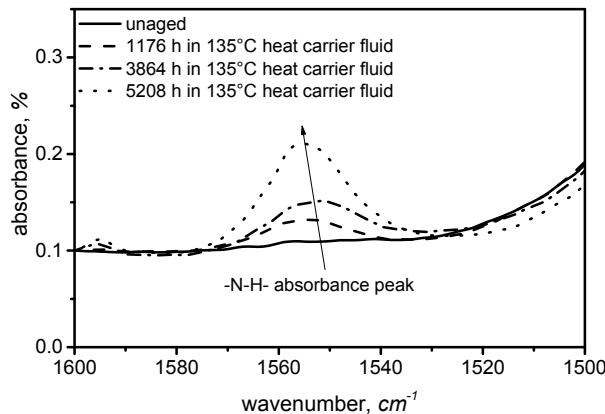


Fig. 10. Effect of hot heat carrier exposure on the formation of a N-H peak in the region from 1530 to 1570  $\text{cm}^{-1}$  for PP-B1.

## Acknowledgements

This research work was performed in the cooperative research projects SolPol-1/2 and SolPol-4/5 entitled "Solar-thermal systems based on polymeric materials" ([www.solpol.at](http://www.solpol.at)). This project is funded by the Austrian Climate and Energy Fund (KLI:EN) within the programme "Neue Energien 2020" and administrated by the Austrian Research Promotion Agency (FFG). The authors wish to express their acknowledgements to Susanne Kahlen, Kurt Stubenrauch and Andreas Meinecke (Borealis, Linz, A) for the cooperation, especially for making available the compounds.

## References

- [1] Allen, N.S., Moore, L.M., Marshall, G.P., Vasiliou, C., Kotecha, J., Valange, B., 1990. Diffusion and extractability characteristics of antioxidants in blue polyethylene water pipe: A DSC and radiolabelling study. Polymer Degradation and Stability 27 (2), 145–157.

- [2] Beißmann, S., Stifflinger, M., Grabmayer, K., Wallner, G., Nitsche, D., Buchberger, W., 2013. Monitoring the degradation of stabilization systems in polypropylene during accelerated aging tests by liquid chromatography combined with atmospheric pressure chemical ionization mass spectrometry. *Polymer Degradation and Stability* 98 (9), 1655–1661.
- [3] Bird, R.E., Hulstrom, R.L., Lewis, L.J., 1983. Terrestrial solar spectral data sets. *Solar Energy* 30 (6), 563–573.
- [4] Celina, M., Gillen, K.T., Assink, R.A., 2005. Accelerated aging and lifetime prediction: Review of non-Arrhenius behavior due to two competing processes. *Polymer Degradation and Stability* 90 (3), 395–404.
- [5] Celina, M.C., 2013. Review of polymer oxidation and its relationship with materials performance and lifetime prediction. *Polymer Degradation and Stability* 90 (3), 395–404.
- [6] Chrissafis, K., Paraskevopoulos, K.M., Stavrev, S.Y., Docolis, A., Vassiliou, A., Bikaris, D.N., 2007. Characterization and thermal degradation mechanism of isotactic polypropylene/carbon black nanocomposites. *Thermochimica Acta* 465 (1–2), 6–17.
- [7] Dörner, G., Lang, R.W., 1998. Influence of various stabilizer systems on the ageing behavior of PE-MD—I. Hot-water ageing of compression molded plaques. *Polymer Degradation and Stability* 62 (3), 421–430.
- [8] Dörner, G., Lang, R.W., 1998. Influence of various stabilizer systems on the ageing behavior of PE-MD—II. Ageing of pipe specimens in air and water at elevated temperatures. *Polymer Degradation and Stability* 62 (3), 431–440.
- [9] Gill, T.S., Knapp, R.J., Bradley, S.W., Bradley, W.L. 1998. Long term durability of cross-linked polyethylene tubing used in chlorinated hot water systems. Presented at ANTEC, Atlanta, Georgia.
- [10] Grein, C., Plummer, C.J.G., Kausch, H.H., Germain, Y., Beguelin, Ph., 2002. Influence of  $\square$  nucleation on the mechanical properties of isotactic polypropylene and rubber modified isotactic polypropylene. *Polymer* 43, 3279–3293.
- [11] Hillerns, F., 2013. Personal communications.
- [12] Horrocks, A.R., Mwila, J., Mirafab, M., Liu, M., Chohan, S.S., 1999. The influence of carbon black on properties of orientated polypropylene 2. Thermal and photodegradation. *Polymer Degradation and Stability* 65 (1), 25–36.
- [13] Huan, Q., Zhu, S., Ma, Y., Zhang, J., Zhang, S., Feng, X., Han, K., Yu, M., 2013. Markedly improving mechanical properties for isotactic polypropylene with large-size spherulites by pressure-induced flow processing. *Polymer* 54 (3), 1177–1183.
- [14] Kahlen, S., Wallner, G.M., Lang, R.W., 2010. Aging behavior and lifetime modeling for polycarbonate. *Solar Energy* 84 (5), 755–762.
- [15] Kahlen, S., Wallner, G.M., Lang, R.W., 2010. Aging behavior of polymeric solar absorber materials – Part 2: Commodity plastics. *Solar Energy* 84 (9), 1577–1586.
- [16] Kurzbock, M., Wallner, G.M., Lang, R.W., 2012. Black pigmented polypropylene materials for solar absorbers. *Energy Procedia* 30 (0), 438–445.
- [17] Mantell, S.C., Davidson, J.H., 2012. Polymer Durability for Solar Thermal Applications, in: Köhl, M., Meir, M. G., Papillon, P., Wallner, G. M., and Saile, S. (Eds.), *Polymeric Materials for Solar Thermal Applications*, First Edition. Wiley-VCH Verlag GmbH & Co. KGaA, 187–210.
- [18] Vibien, P., Couch, J., Oliphant, K., 2001. Chlorine resistance testing of cross-linked polyethylene piping materials. Presented at ANTEC, Dallas, TX.
- [19] Wallner, G.M., Grabmayer, K., Beißmann, S., Schobermayr, H., Buchberger, W., Lang, R.W., 2013. Methoden zur beschleunigten Alterungsprüfung von Kunststoffen. *Erneuerbare Energie* 2013-1, 18–20.
- [20] Wise, J., Gillen, K.T., Clough, R.L., 1997. Time development of diffusion-limited oxidation profiles in a radiation environment. *Radiation Physics and Chemistry* 49 (5), 565–573.